This material has been copied
under licence from CANCOPY.
Resale or further copying of this material is
strictly prohibited.

Le présent document a été reproduit
avec l'autorisation de CANCOPY.
La revente ou la reproduction ultérieure
en sont strictement interdites.

PNC-N341 76-09

PRESENTED AT JOINT MEETING OF
AMERICAN NUCLEAR SOCIETY AND
CANADIAN NUCLEAR ASSOCIATION,
TORONTO, JUNE 13-18, 1976

NUCLEAR DESIGN AND ITS DEVELOPMENT FOR FUGEN

June, 1976

Hidemasa KATO

Yoshio MIYAWAKI

Power Reactor and Nuclear Fuel
Development Corporation, Japan

Nuclear Design and Its Devleopment for FUGEN

I. Introduction

The purpose of this study is to confirm the validity of the nuclear design for a heavy water moderated, boiling light water cooled, pressure tube type reactor, FUGEN[1], which is now under construction in Japan.

The reactor, FUGEN will use Pu mixed-oxide fuel, and interest centers on the effectiveness of such fuel. This type of reactor can be efficiently operated on mixed oxide fuel or slightly enriched U oxide fuel, using the same lattice and the same shaped fuel assemblies. The use of Pu fuel is expected to have a favorable effect also on the coolant void coefficient, thus raising the level of reactor safety and stability.

II. FUGEN Nuclear Design

The core configuration of FUGEN is shown in Fig. 1. In the initial core of FUGEN, ninety-six mixed oxide fuel assemblies will be loaded in the center region and one hundred twenty eight slightly enriched (1.5 %) U oxide fuel assemblies in the surrounding region. The amount of Pu in the initial core is almost the same as in the equilibrium core, with the result that the void coefficient will change little throughout the reactor life.

A cross-sectional view of a FUGEN fuel assembly is shown in Fig. 2. In order to reduce the local power peaking in the

fuel assembly, the fissile Pu content of the mixed oxide is set at 0.55 wt % for sixteen rods of the outer ring and 0.8 wt % for twelve rods of the middle and the innermost rings.

Figure 3 shows calculated coolant void reactivities for the Fugen design. The zero point of the reactivity is set at 35 % of coolant void on the normal operating condition. Two solid line curves show the void reactivities of 1.5 % enriched UO_2 and the mixed oxide cores, respectively. For the initial core of FUGEN, the dotted line curves are expected. In the initial core, some control rods will be inserted. Thus, the void coefficient will be slightly more negative side, with the effect of control rods, as explained later.

Figure 4 shows calculated local power peaking factors of FUGEN fuel assemblies. The local power peaking factor is improved 5 % lower in the mixed oxide fuel assembly than that in the 1.5 % enriched UO_2 fuel assembly.

The principal criteria of FUGEN nuclear design are briefly as follows:

1) The power coefficient should be negative.
2) The maximum power peaking should be below 2.1.
3) The minimum critical heat flux ratio should be above 1.9.

In order to meet these criteria, the control rod sequence has been designed, on the basis of a three dimensional thermo-nuclear code LAYMON, an improved version of the FLARE code[2], which was developed for this type of reactors. An adequate control rod sequence for the initial fuel cycle has been determined on Hailing's principle[3]. In this sequence, at the change-over from the initial core, all control rods will be

withdrawn except the power regulating rods for operation, maintaining the gross peaking factor within the limit of the criteria, allowing for the design margin.

Figure 5 shows a typical example of the calculated channel power, burn up, and channel flow distributions, and minimum critical heat flux ratio by channel for the FUGEN reactor. In this control rod sequence, two kinds of control rod patterns were used, as shown number (11) and (13), with various depth of insertions. The number means depth of control rod insertion. (16 is full out and 0 is full in.) In this figure, MCHFR is greater than 2.6, at the full power condition. Figure 6 illustrates the calculated radial power distribution at approximately 6,000 MWD/TU of the exposure. Figure 7 shows the axial power distribution at the same exposure as before. Figure 8 shows the change of the radial power distribution with exposure.

The nuclear design[4-6] of FUGEN has been checked, using our nuclear design codes, by experiments[7-11] with our Deuterium Critical Assembly (DCA). In order to evaluate the details of the Pu fueled core, a CLUSTER-code[12] has been developed, based on the collision probability method. The LAYMON code was also checked in DCA experiments.

III. Pu Effect on Void Coefficient

The physical meaning of Pu effect on the void coefficient has been investigated, previously.[4,6] In the study, two kinds of fuels, mixed oxide and slightly enriched UO_2 fuels, for a

28 rod cluster were selected for a comparison case. Table 1 shows the fuel composition of the comparison case. Details of the comparison case are given in the appendix. Weight fraction of the fissile Pu in this mixed oxide fuel is 0.54 %. Thus, the weight fraction of total fissile isotopes is 1.25 % in the Pu fuel and 1.5 % in the U fuel. Therefore, the fissile content in the Pu fuel is less than that in the U fuel.

Figure 9 illustrates the calculated K_{eff} and K_∞ on the comparison case. The calculations with METHUSELAH and MINI-WIMS codes have been carried out in the United Kingdom following our input specification. The calculation with CLUSTER-code was performed in Japan. These three calculations show that the increase of K_∞ and K_{eff} with coolant void fraction is less in the mixed oxide core, than in the UO_2 core.

Table 2 shows the variation of the effective absorption cross section of each isotope with void fraction for the comparison case. In this table, we notice that the changes of the effective absorption cross sections of Pu^{239} and Pu^{241} are negative at the full void, while the changes on the other isotopes are positive.

To study the reason why the effective absorption cross section of Pu^{239} and Pu^{241} is lower at large void fraction, spectral indices were defined. S_1 is the ratio of fast and thermal fluxes. S_2 is the ratio of higher and lower energy component in the thermal flux. From Fig. 10, it is found that S_2 in fuel region becomes lower as coolant void fraction increases, in both the UO_2 and the mixed oxide cores. This means that the thermal neutron spectrum in the fuel region becomes

softer as coolant void fraction increases. It is also found that S_2 in fuel is two times greater than that in D_2O at the lower coolant void fraction. This means that thermal neutron spectrum in the fuel channel is harder than that in D_2O in reactor operating condition.

Figure 11 illustrates the thermal neutron spectrum in the mixed oxide lattice. It is found that thermal neutron spectrum in fuel region is harder than in moderator region, and the spectrum in fuel at full void is softer than that at 35 % void fraction. This spectrum shift results in the larger contribution of the neutron current from D_2O region in the larger void condition. This neutron spectrum shift contributes to the decrease of the reaction rates of Pu^{239} and Pu^{241}, since they both have a large resonance at 0.3 eV in thermal energy region.

Here is one reason why Pu suppresses coolant void coefficient, which results in the larger Pu cross-section, compared with U cross-section. Table 3 shows a comparison of macroscopic absorption corss section of fuel and coolant. In the mixed oxide lattice, the contribution of coolant is less than in the UO_2 lattice.

The two effects mainly contribute to the coolant void coefficient in the mixed oxide core, and almost the same magnitude in this comparison case.

IV. DCA Experiment

First, we describe the experimental verification of Pu effect on the void coefficient. Figure 12 shows experiment on coolant void reactivity of DCA. The upper solid curve shows experiment on 1.2 % enriched UO_2 core. And, the lower solid curve shows experiment on mixed oxide fuel loaded core, in which twenty five mixed oxide fuel assemblies are loaded, surrounded by ninety six UO_2 fuel assemblies as shown in Fig. 13. Total Pu content in the mixed oxide fuel is 0.54 % (the fissile Pu isotope content is 0.49 %). Therefore, the contents of fissile isotopes in both the UO_2 fuel and the mixed oxide fuel are almost equal. Dotted line curves show calculation by METHUSELAH and try angular marks at the full void show calculation by CLUSTER-code. From these results, it is found that Pu is effective in reducing the void coefficient.

Now, we describe control rod worth of mixed oxide fuel loaded core. Table 4 shows a typical experiment result of control rod worth in the two region core of DCA with twenty five mixed oxide fuel assemblies surrounded by ninety six UO_2 fuel assemblies. The calculation of control rod worth was performed with the absorption area method. In 0 % void, calculation agrees with experiment satisfactorily. In full void, control rod worth is underestimated. Especially, the discrepancy is larger in the case of many control rod insertions at full void in mixed oxide core, the discrepancy in such case is almost 20 %.

Table 5 shows another experiment on control rod worth in DCA with 1.2 % enriched UO_2 core. In this experiment, changes

of control rod reactivity worth with coolant void fraction were studied. We notice that the control rod reactivity worth increases in the large coolant void fraction of 70 % and 100 %. Figure 14 illustrates the coolant void dependency on the control rod reactivity. From this result, it is found that control rod effect also contributes to the suppression of void coefficient. This effect results from the reason that neutron migration area becomes large in the large void fraction, and the neutron absorption by control rods becomes large.

Now, we describe the accuracy of estimation of power distribution. Figure 15 shows a typical example of the core configuration of DCA experiment, with checkerboard core, using three kinds of fuels, 0.54 % (0.49 % of fissile Pu) and 0.87 % (0.79 % of fissile Pu) mixed oxide fuels, and 1.2 % enriched UO_2 fuel, for simulating refueling core. Figure 16 shows a typical example of the experiment result and the calculation. This shows the radial flux distribution of the checkerboard core, with four control rod insertions. This shows a quarter section. This calculation was performed using the LAYMON code. The discrepancy between the experiment and the calculation on the radial flux distribution was evaluated as approximately 5 % at peak channel by root mean square, through the analysis of three kinds of cores (mixed oxide core, UO_2 core, and checkerboard core).

The accuracy of the calculation on the local power peaking factor was evaluated by experiments in DCA. Discrepancy between the experiment and the calculation was found to be almost 1 % on the peaking factor for both the mixed oxide and U oxide fuel assemblies.

V. Conclusion

FUGEN nuclear design with Pu fuel loading has been checked, by DCA experiment, using various nuclear design codes. Especially, both by experiment and calculation, it has been shown that Pu is effective in reducing the void coefficient. Neutron absorption effect by control rods also contributes to reduce the void coefficient.

And, further experiment are now in progress with mixed oxide fuel cores in DCA in preparation for refueling and for the evaluation of future plants. FUGEN is expected to be in operation in 1978. And, more information will be presented in the near future.

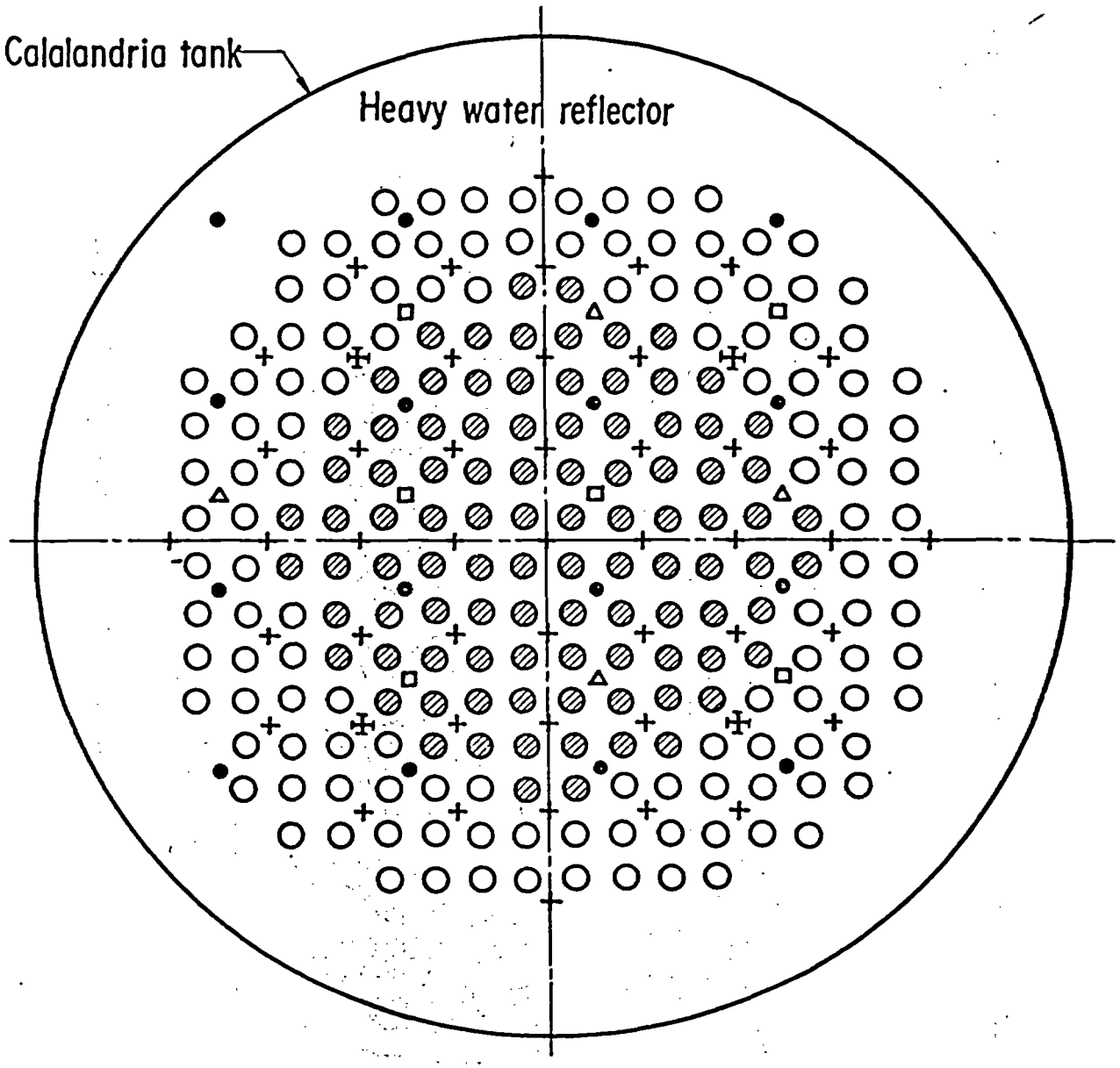

○	FUEL ASSEMBLY UO_2	128	•	LPM	16x4
⊘	PuO_2-UO_2	96	□	PUM	6
+	CONTROL ROD	45	△	SUM	4
✠	REGULATING ROD	4			

Fig. 1 CORE CONFIGURATION OF FUGEN (INITIAL LOADING)

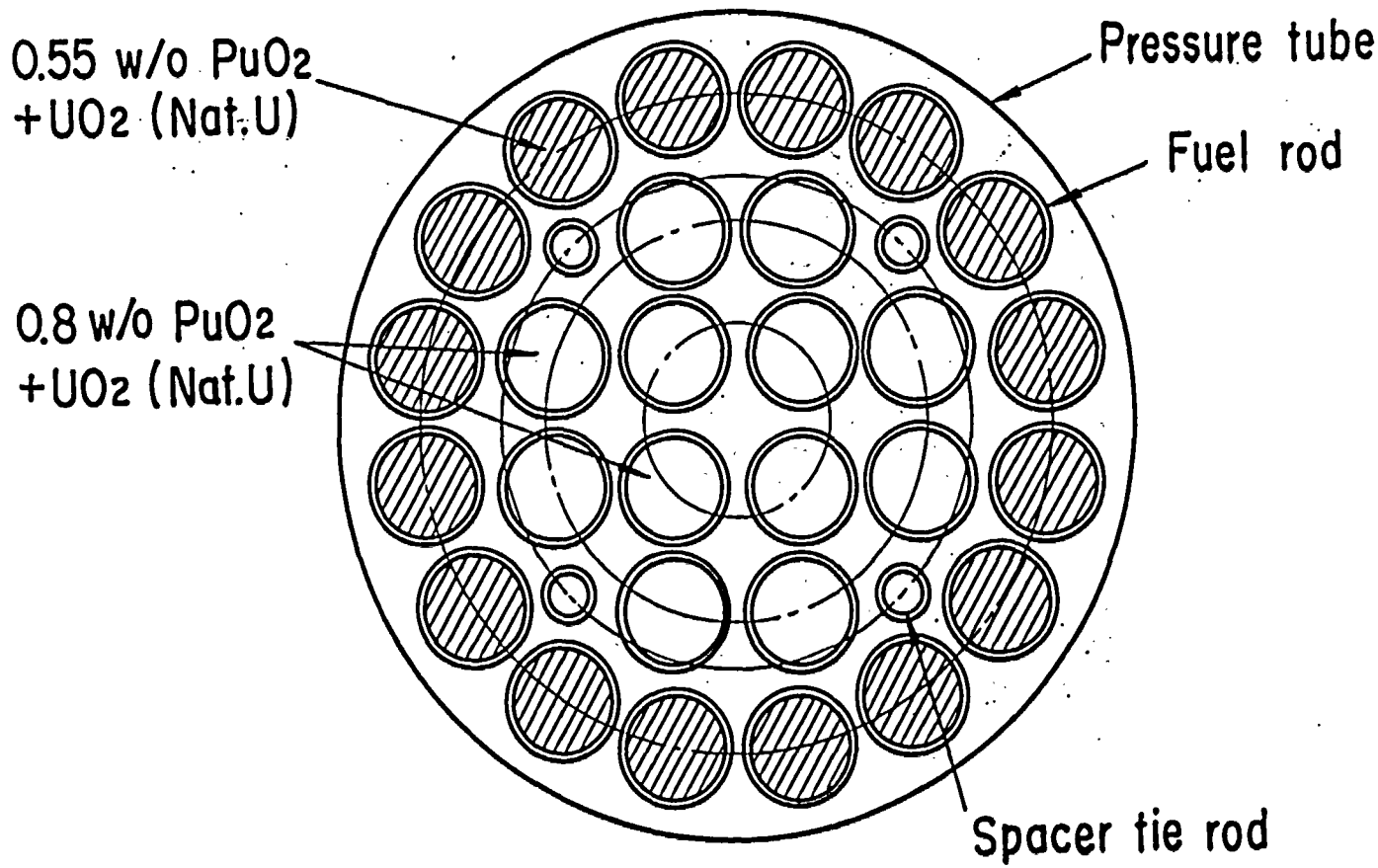

Fig.2 Mixed Oxide Fuel Assembly of FUGEN

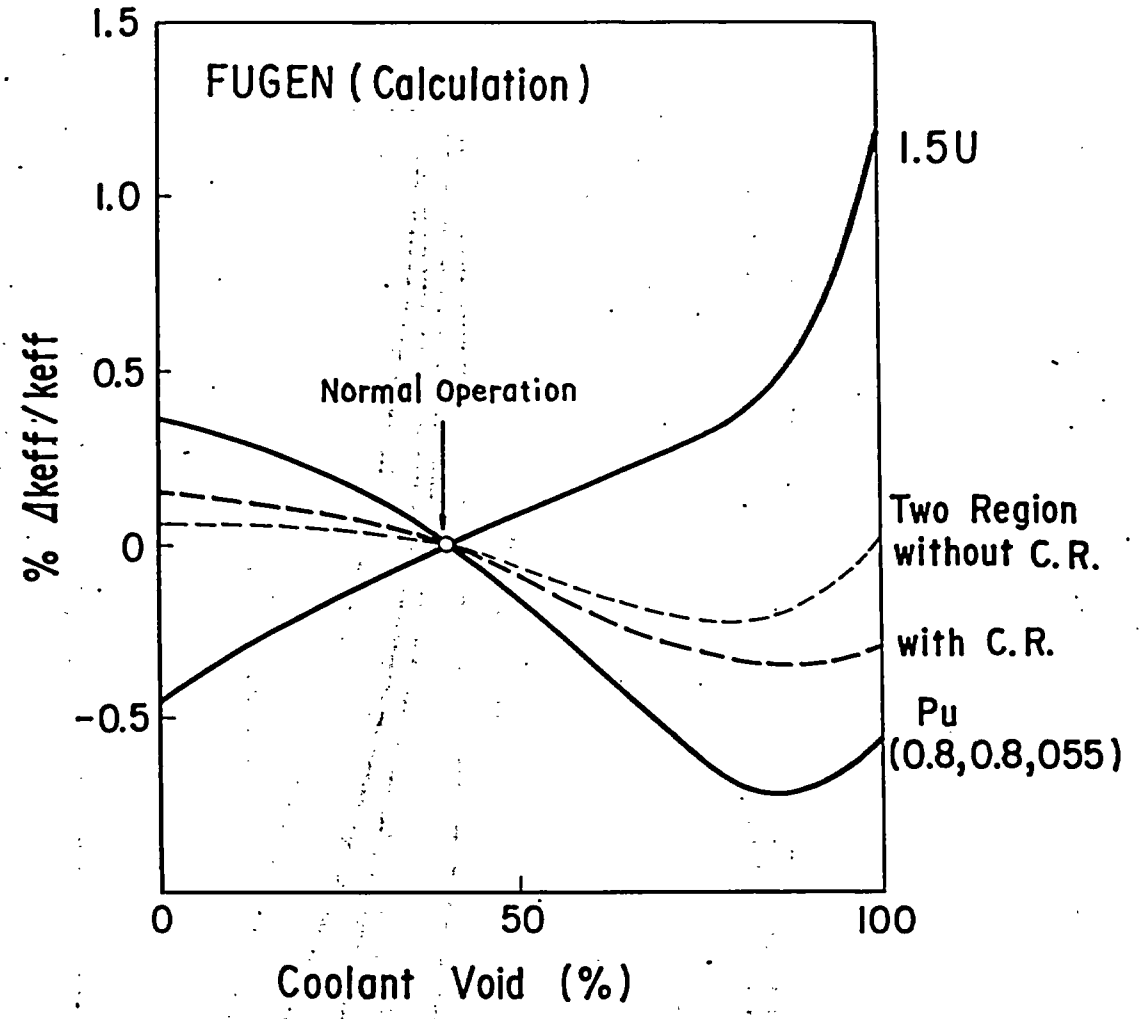

Fig.3 Change of Coolant Void Reactivity for FUGEN at BOC
((0.8,0.8,0.55) PuO_2-UO_2 Lattice, 1.5 Enriched UO_2 Lattice and the Two Region Core)

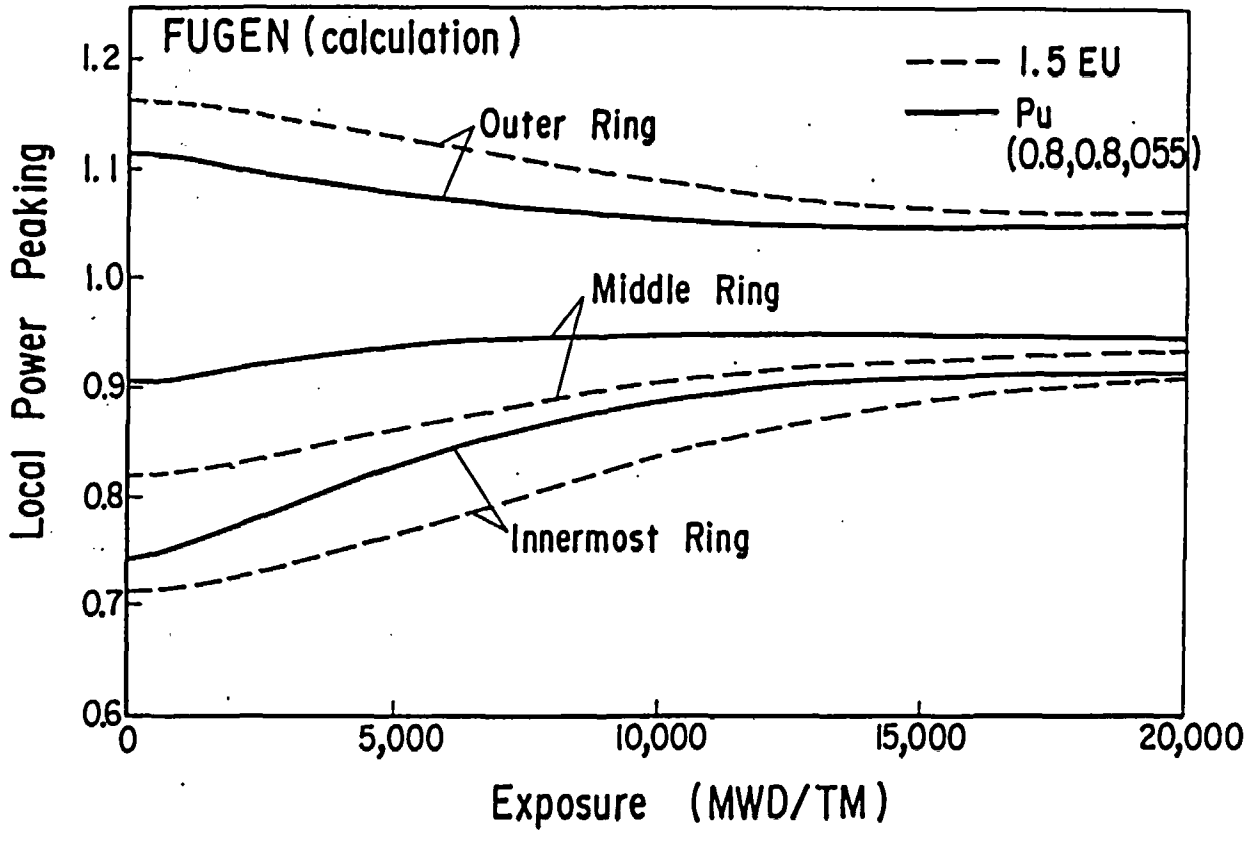

Fig. 4 Change of Local Power Peaking with Burn Up

J

I

RELATIVE POWER				0.885	0.965	0.990	0.997	4.969	4.865	4.546	3.814	EXPOSURE (GWD/T)			
		0.878	0.971	1.050	1.081	1.085	1.085	6.354	6.297	6.028	5.466	4.565	3.648		
	0.979	1.022	1.064	1.079	1.080	1.041	1.032	6.579	6.904	6.749	6.315	5.135	4.968	3.643	
	0.974	1.066	1.029	1.009	1.009	0.996	0.976	6.384	6.682	6.632	6.366	6.039	5.724	4.553	
			(11)				(13)				(11)				
0.990	1.056	1.035	1.012	0.949	0.978	0.966	0.956	6.153	6.514	6.620	6.178	6.352	6.287	5.439	3.792
0.971	1.091	1.094	1.016	0.980	0.904	0.933	0.965	5.735	6.085	6.179	6.608	6.600	6.691	5.984	4.517
					(11)				(11)						
0.996	1.098	1.085	1.008	0.970	0.934	0.923	0.960	5.622	5.781	6.080	6.497	6.635	6.563	6.241	4.836
1.000	1.090	1.040	0.980	0.958	0.966	0.960	0.943	5.853	5.622	5.733	6.146	6.368	6.546	6.334	4.957
			(13)				(13)				(13)				
3.334 2.618	3.312 2.654	3.458 2.788	3.508 2.845	3.463 2.803	3.363 2.729	3.330 2.698	3.336 2.705	1.101	1.096	1.094	1.096	1.090	1.073	1.059	0.700
3.373 2.651	3.322 2.666	3.454 2.785	3.528 2.859	3.499 2.836	3.386 2.744	3.366 2.728	3.329 2.698	1.096	1.106	1.103	1.093	1.082	1.060	1.057	0.701
					(11)				(11)						
3.497 2.754	3.337 2.687	3.323 2.674	3.465 2.805	3.460 2.802	3.569 2.893	3.382 2.741	3.366 2.728	1.094	1.103	1.093	1.090	1.080	1.058	1.059	0.704
3.916 3.107	3.451 2.781	3.283 2.652	3.300 2.668	3.442 2.788	3.450 2.794	3.483 2.823	3.457 2.802	1.097	1.094	1.091	1.099	1.081	1.061	1.069	0.713
			(11)				(13)					(11)			
	3.478 2.754	3.332 2.693	3.250 2.626	3.290 2.659	3.437 2.782	3.480 2.819	3.491 2.880	1.091	1.086	1.092	1.082	1.076	1.066	0.703	
	3.946 3.147	3.538 2.867	3.325 2.688	3.263 2.635	3.270 2.630	3.288 2.645	3.423 2.759	1.076	1.073	1.062	1.062	1.066	1.078	0.714	
100%POWER 120%POWER		3.941 3.142	3.466 2.745	3.429 2.763	3.301 2.657	3.271 2.621	3.293 2.638	1.061	1.061	1.062	1.070	0.704	0.714		
MCHFR BY CHANNEL				3.889 3.088	3.465 2.727	3.341 2.624	3.321 2.608	0.701	0.701	0.704	0.713	FRACTIONAL FLOW			

(N) : Control rod insertion (16= Full out, 0= Full in)

Fig.5 A Typical Example of Calculated Channel Power Distribution, Burn Up Distribution, Channel Flow Distribution and MCHFR by Channel of FUGEN (By LAYMON-code)

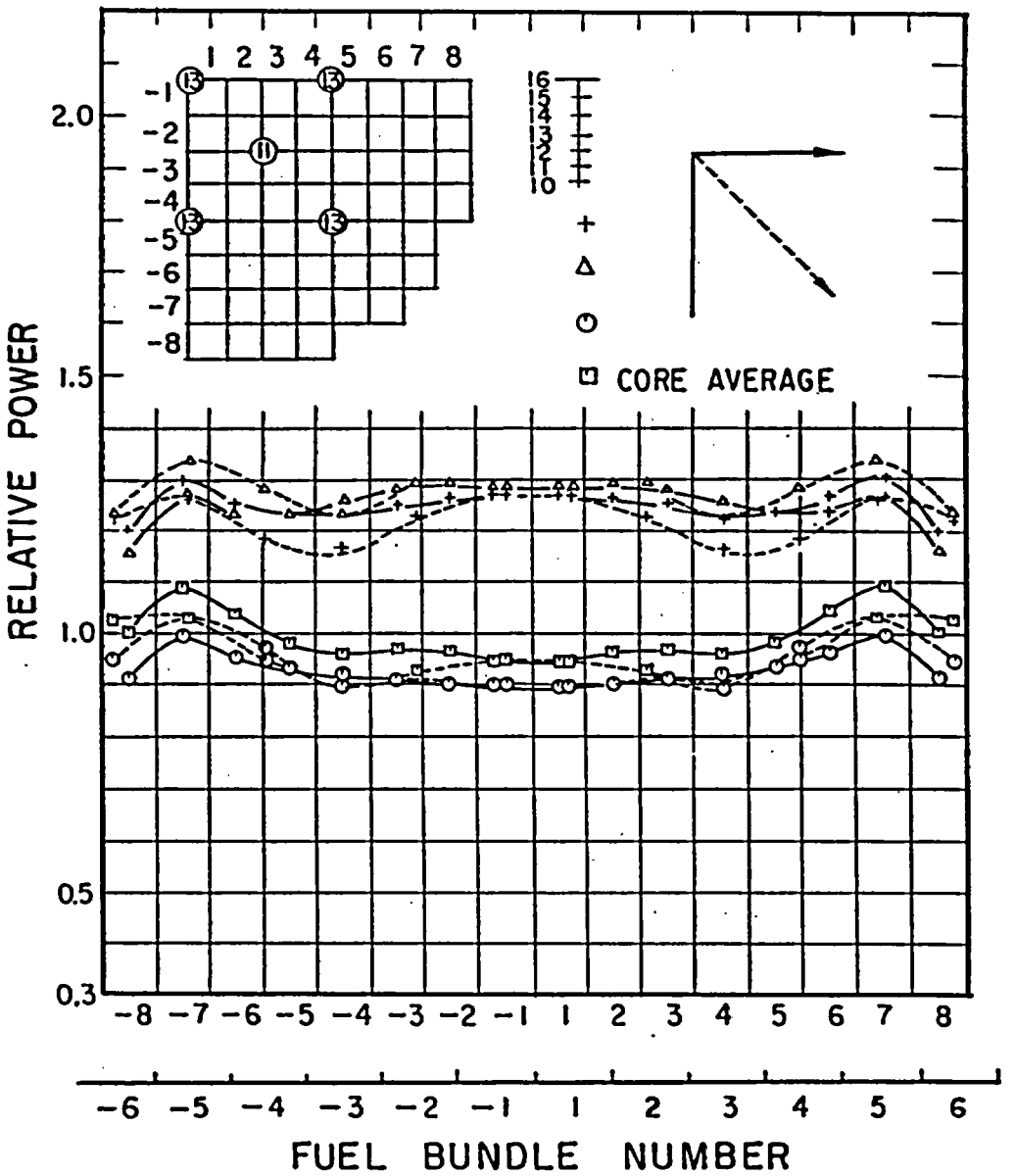

Fig.6 A Typical Example of Radial Power Distribution of FUGEN (Calculation)

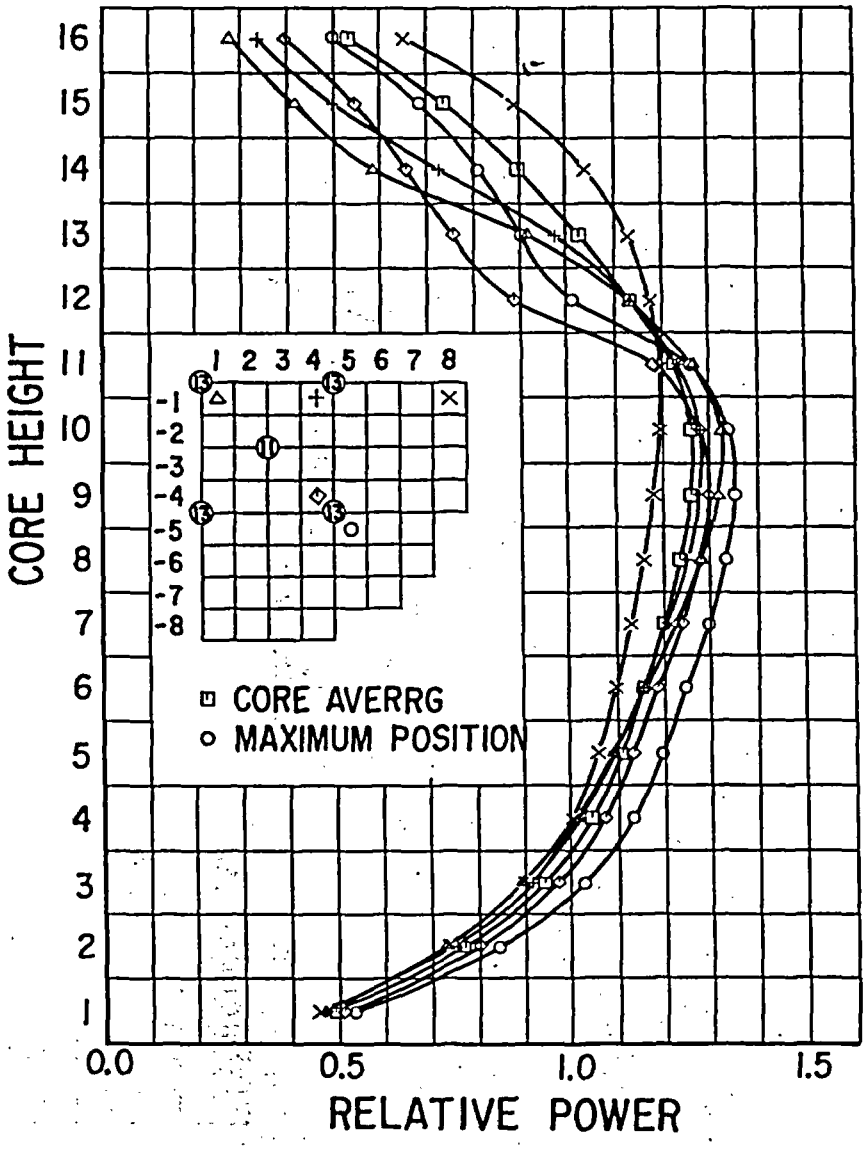

Fig.7 Axial Power Distribution
(Exposre 5.810 GWD/TU)

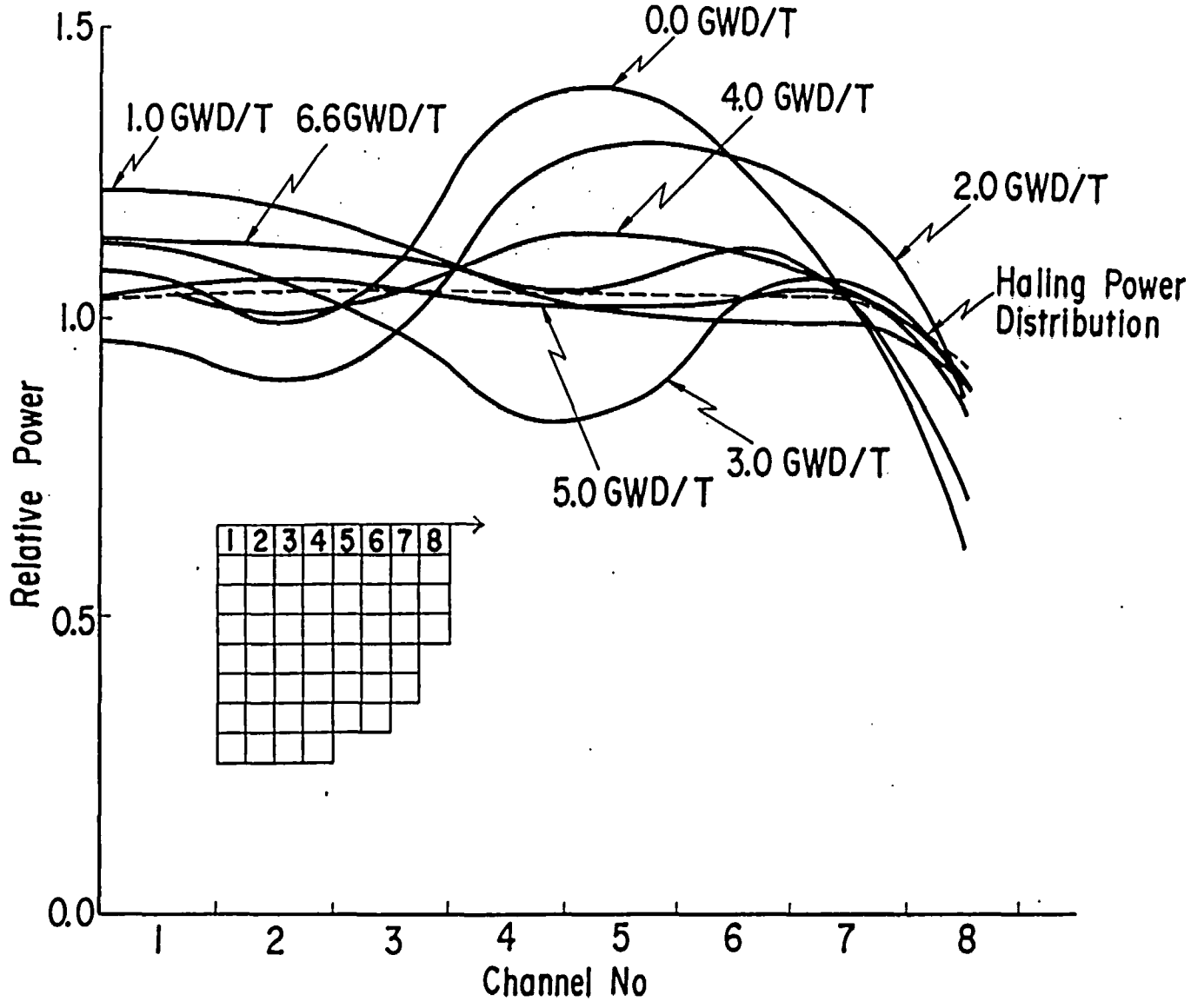

Fig.8 Change of Radial Power Distribution with Burn-Up

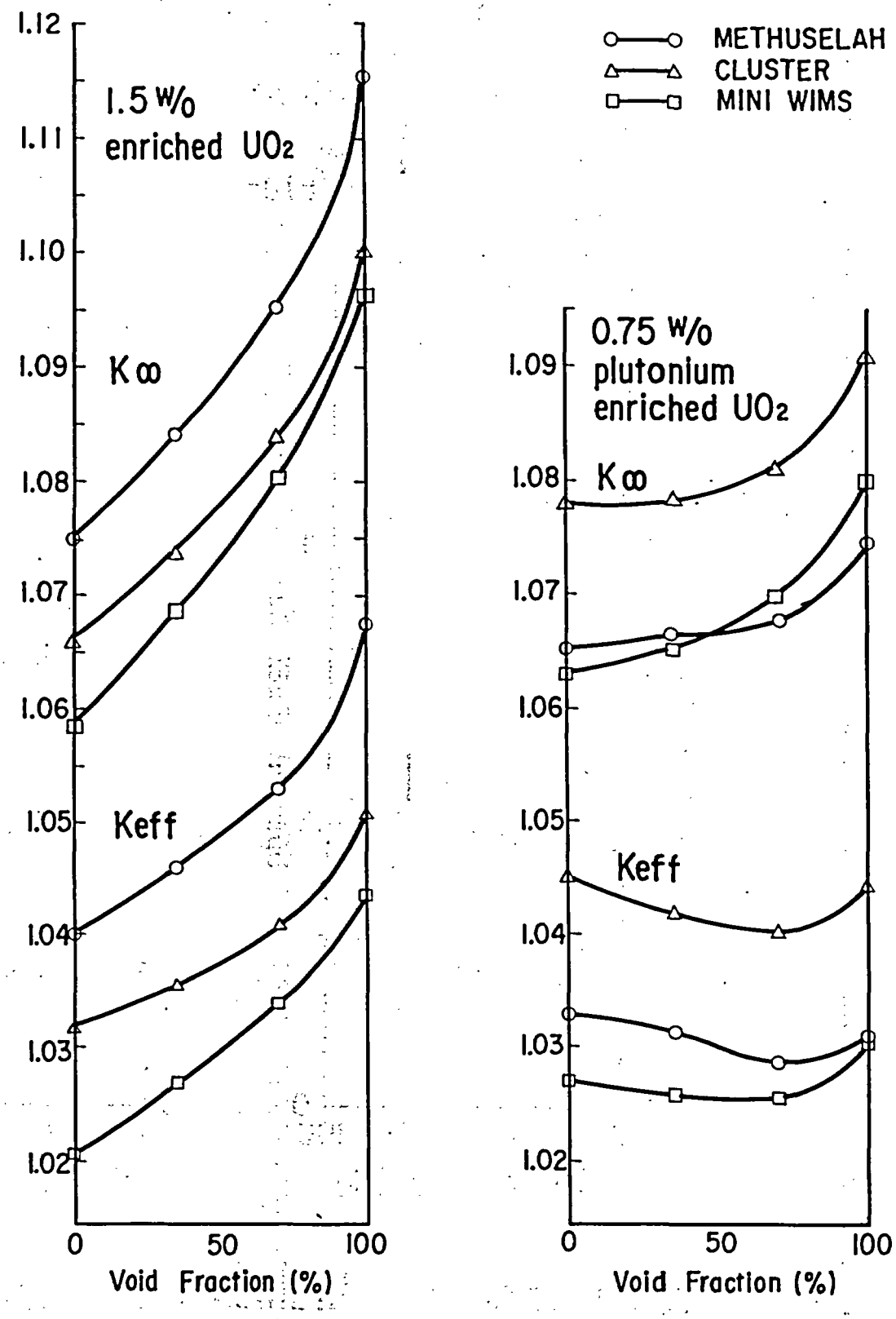

Fig.9 K∞ AND Keff VS COOLANT VOID FRACTION

$$S_1 = \int_{0.625eV}^{\infty} \phi(E)dE \Big/ \int_{0}^{0.625eV} \phi(E)dE$$

$$S_2 = \int_{0.14eV}^{0.625eV} \phi(E)dE \Big/ \int_{0}^{0.14eV} \phi(E)dE$$

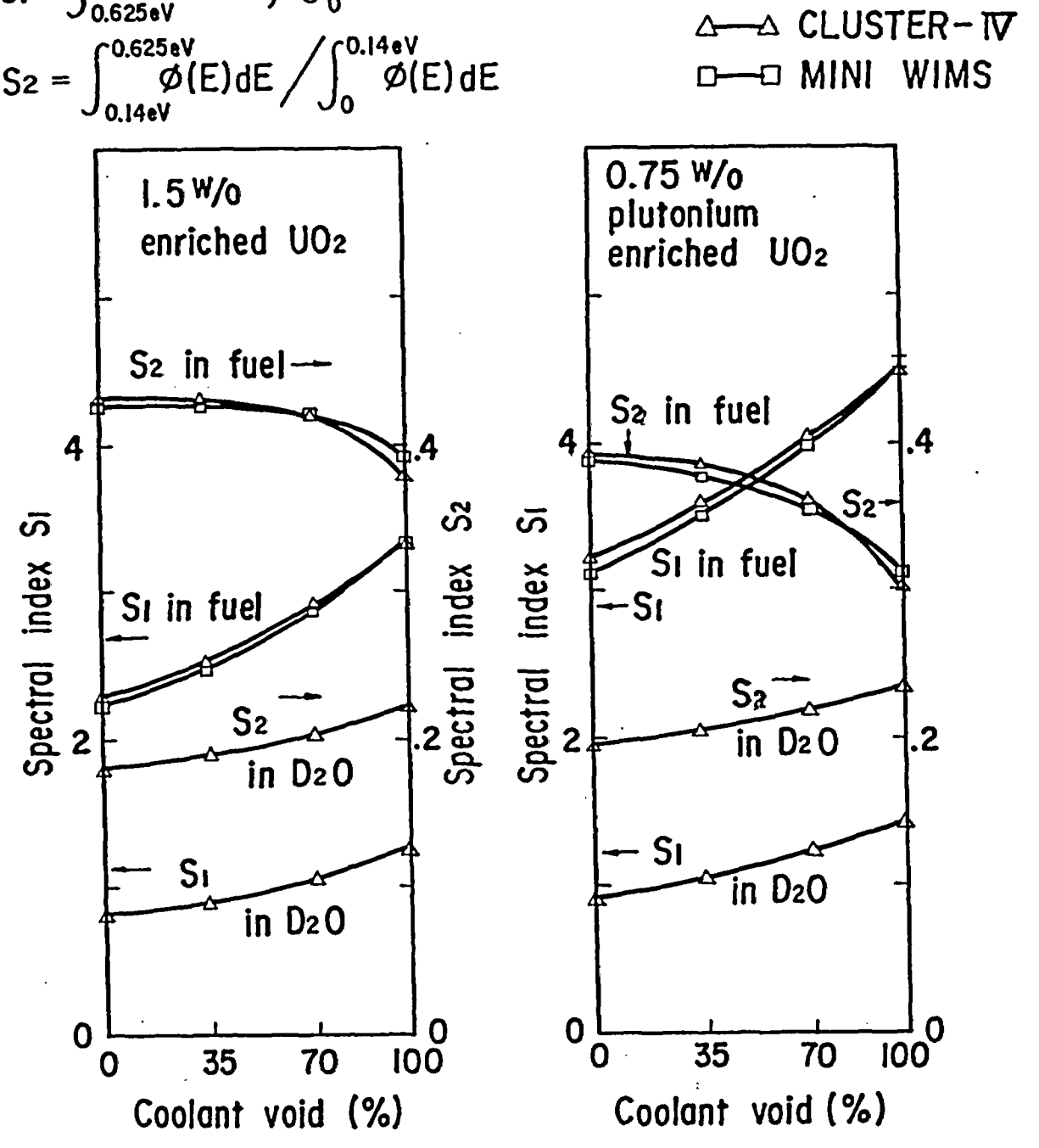

Fig.10 Spectral indices with coolant void fraction (S_1 and S_2 in fuel and in D_2O region)

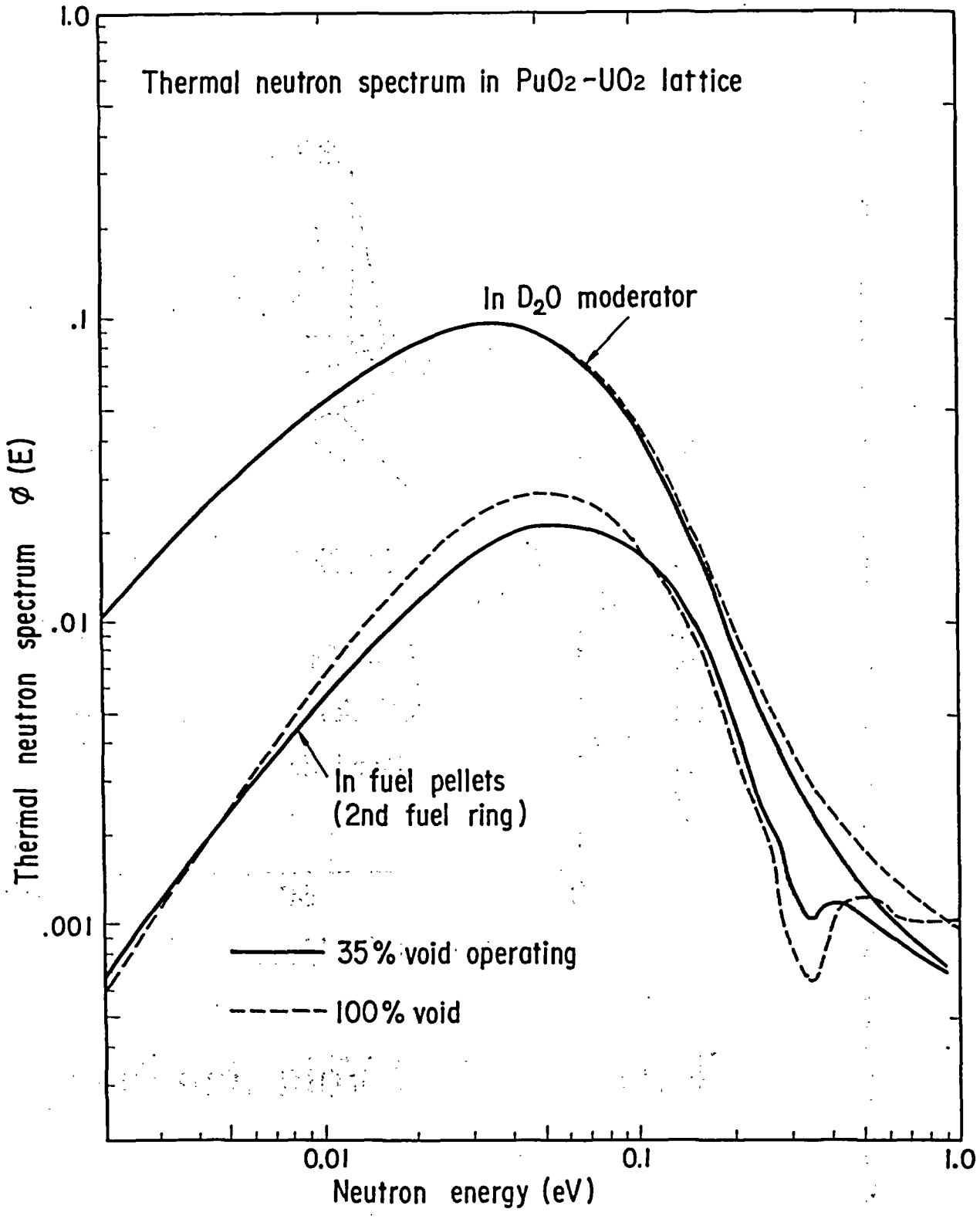

Fig.11 Thermal neutron spectrum in 0.75 % Plutonium enriched PuO_2-UO_2 fuel

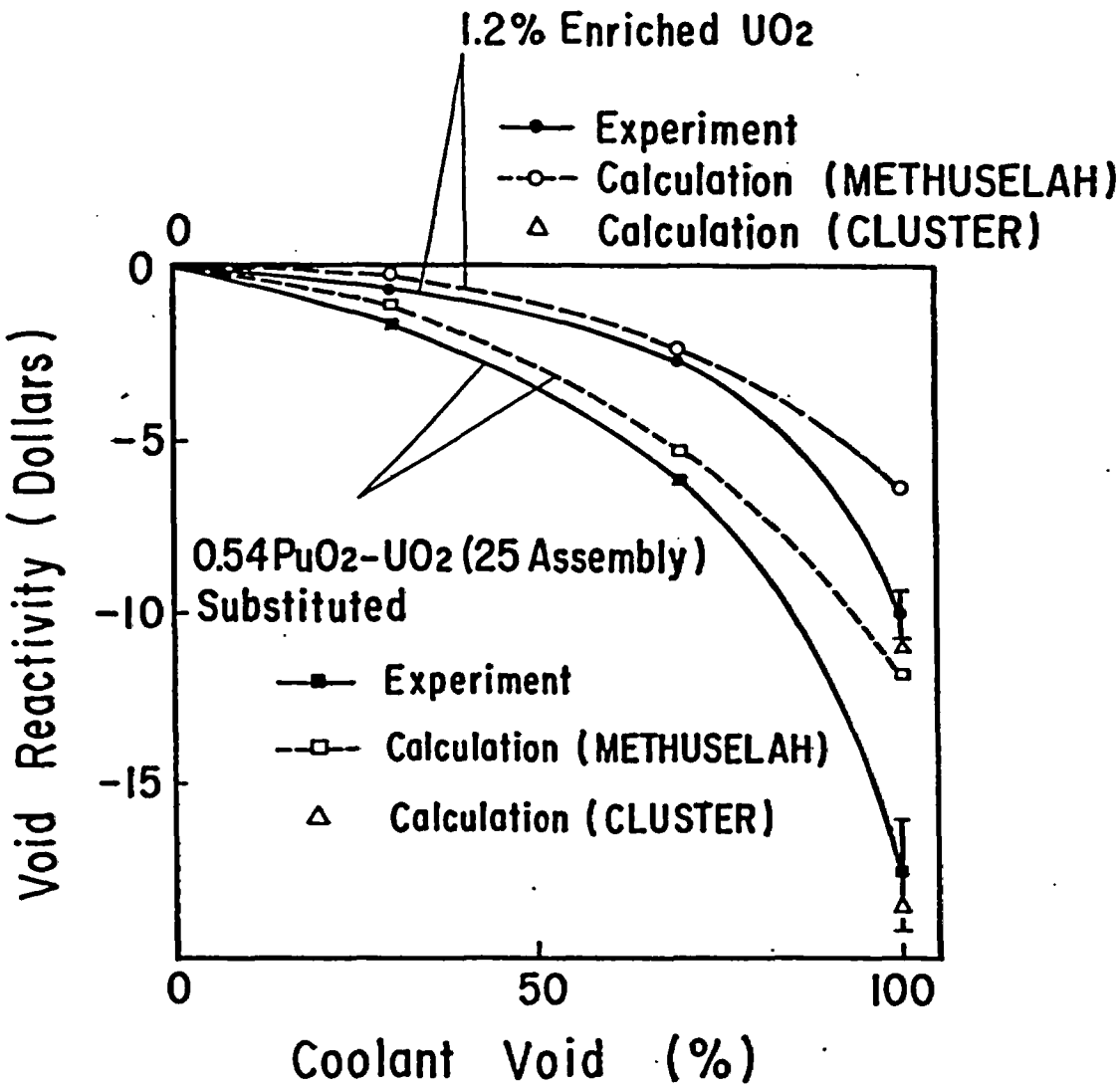

Fig.12 Coolant Void Reactivity of DCA

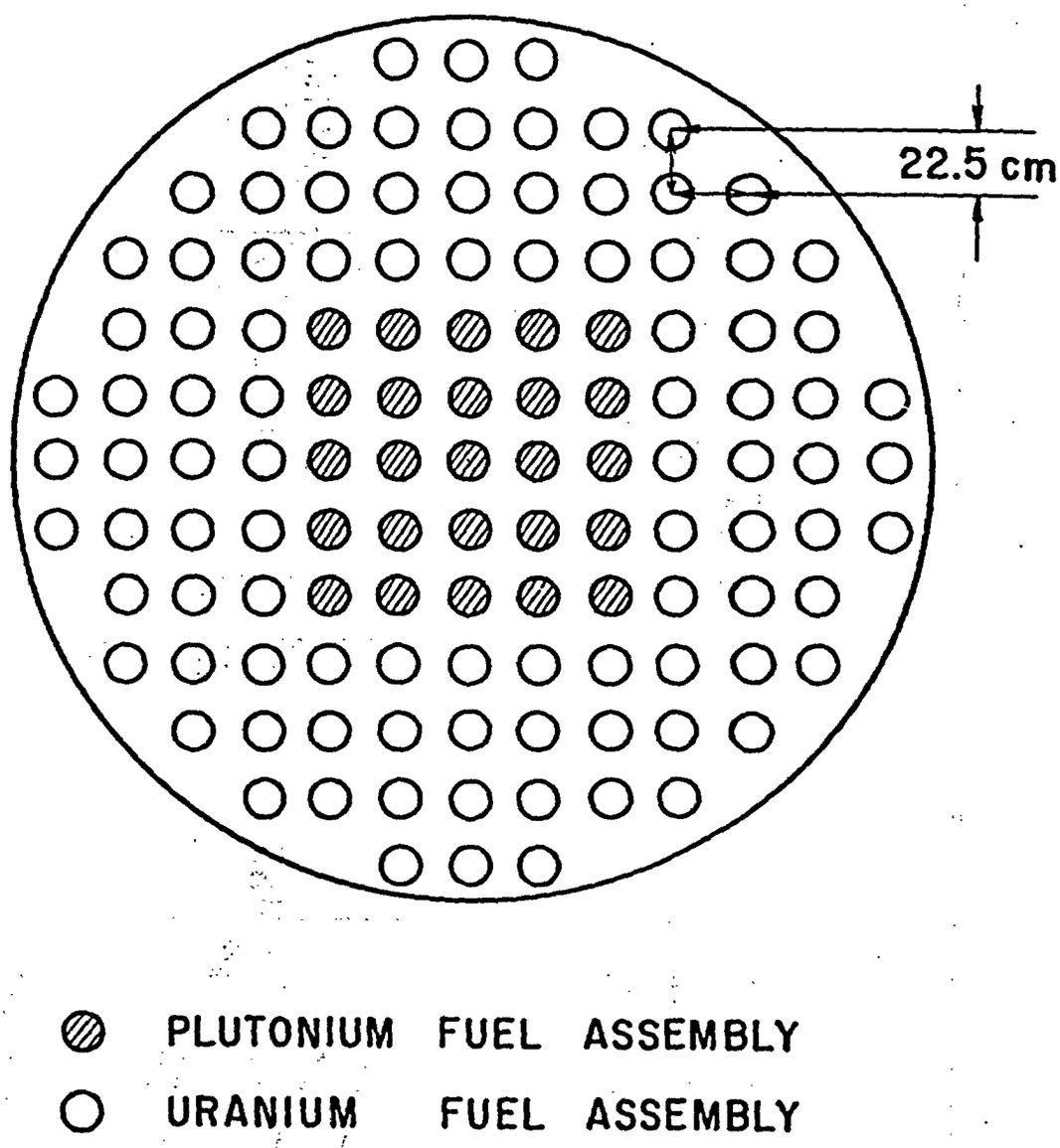

Fig.13 Core Configuration of DCA

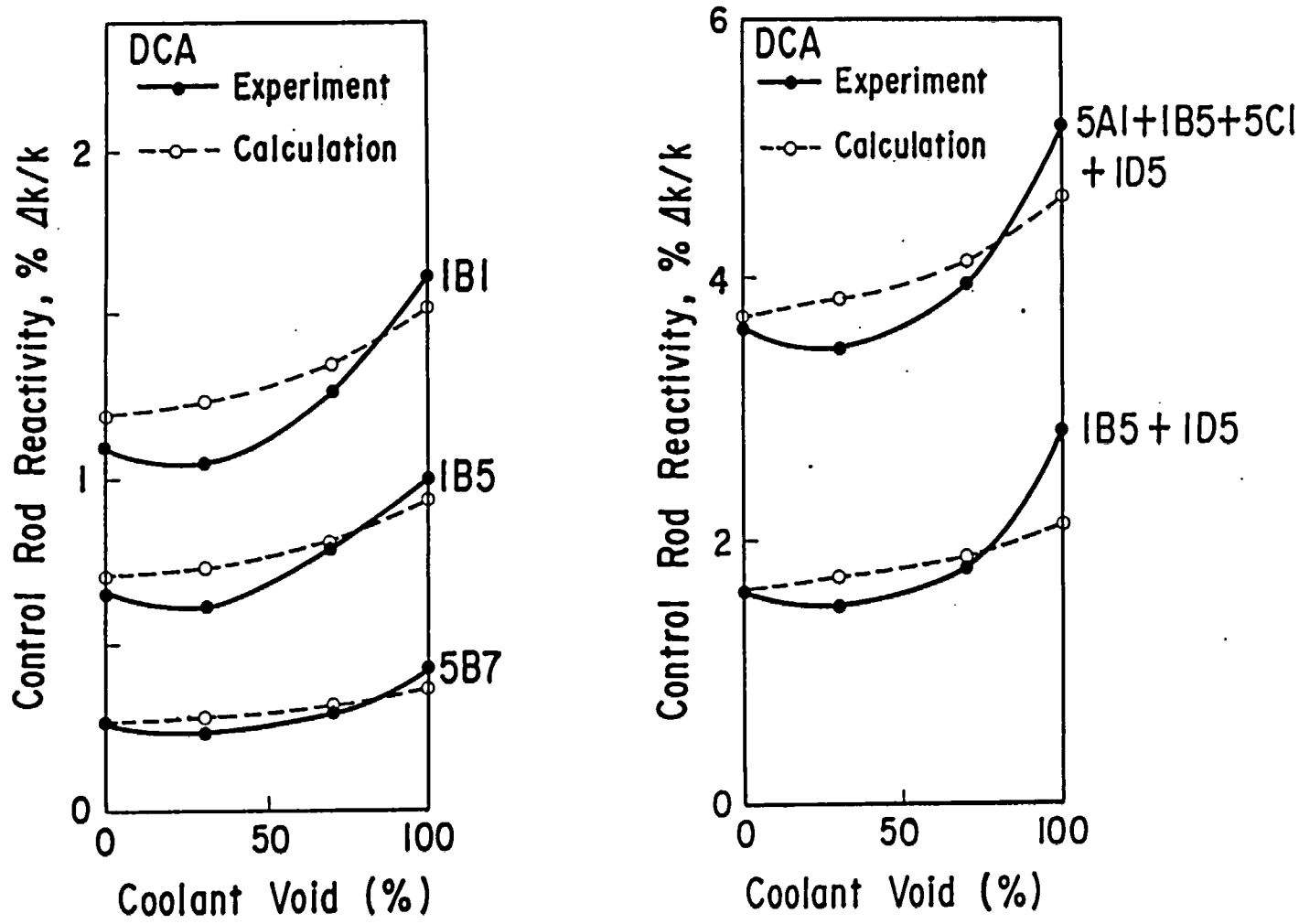

Fig.14 Void dependency of control rod reactivity for DCA core

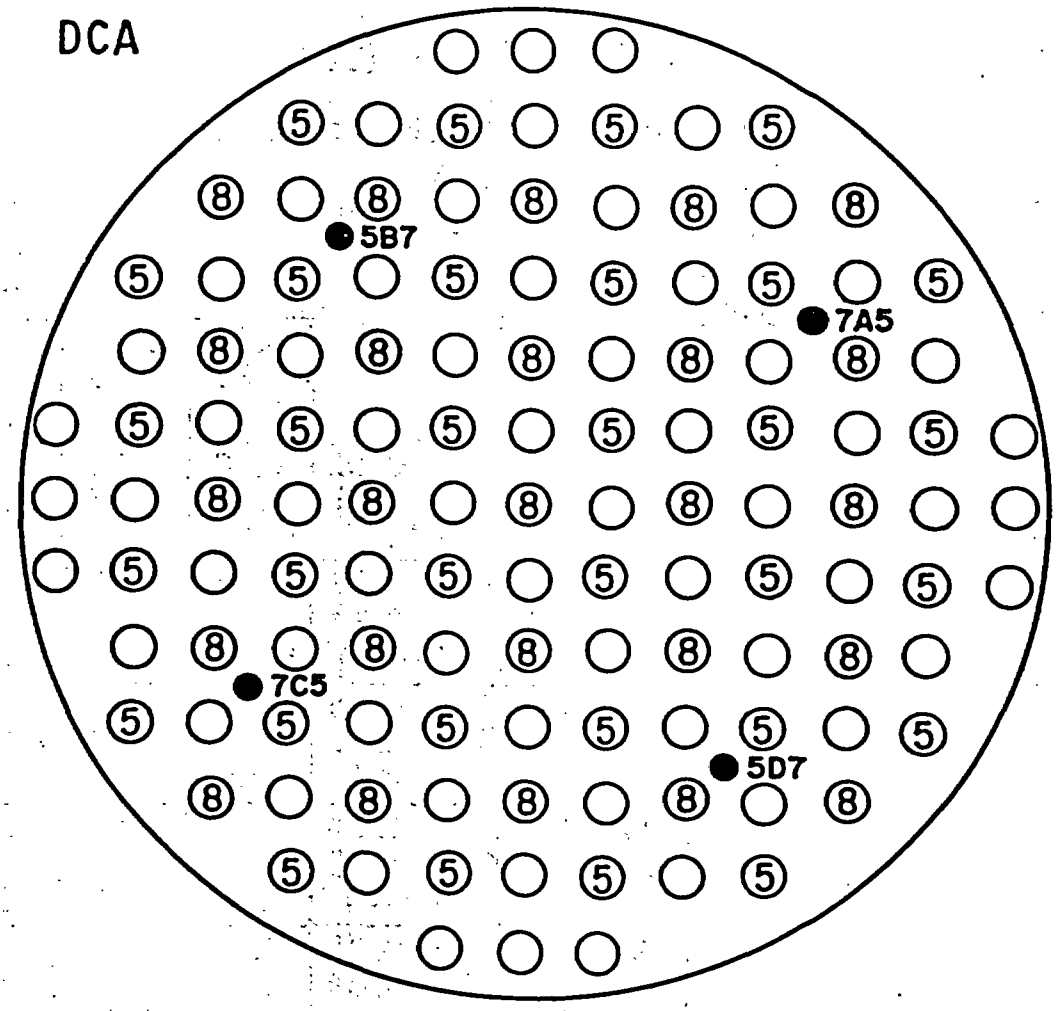

⑤ 0.54 W/o PuO_2–UO_2 (32 Assemblies)

⑧ 0.87 W/o PuO_2–UO_2 (25 Assemblies)

○ 1.2 W/o UO_2 (64 Assemblies)

● Experimental Control Rods

Fig.15 Checkerboad Core with Thirty-Two 0.54 W/o PuO_2-UO_2, Twenty-Five 0.87 W/o PuO_2-UO_2 and Sixty-Four 1.2 W/o UO_2 Fuel Assemblies (DCA)

U, Pu Checkerboard Core (DCA)

0.54 PuO_2–UO_2 : 32 Fuel Assemblies
0.87 PuO_2–UO_2(S): 25
1.2 UO_2 : 64
22.5 cm Lattice Pitch
Coolant Void 0 (%)

					0.26 0.27 4.6	0.29 0.30 4.9
			0.22 0.23 7.4	0.46 0.48 3.5	0.52 0.55 4.5	0.77 0.74 -3.5
		0.23 0.26 13.1	0.46 0.53 15.2	0.46 0.53 14.8	1.07 1.04 -3.1	0.78 0.84 7.8
	0.31 0.29 -6.1	0.66 0.64 -2.0	0.65 0.73 12.5	1.15 1.14 -1.2	1.20 1.25 4.0	1.69 1.64 -2.9
	0.60 0.59 -2.5	0.65 0.66 2.1	1.37 1.29 -6.5	1.13 1.14 0.7	2.00 1.91 -4.4	1.34 1.43 2.5
0.28 0.30 6.5	0.59 0.60 3.1	1.24 1.15 -6.7	1.29 1.33 2.8	2.01 1.95 -3.2	1.84 1.88 2.1	2.25 2.33 3.5
0.31 0.30 -3.8	0.78 0.74 -5.6	0.81 0.84 3.5	1.70 1.64 -3.2	1.34 1.43 7.4	2.42 2.33 -3.7	1.65 1.71 3.6

Exp. Cal. Erorr

Exp. : Experimental Value
Cal. : Calculational Value
Error = {(Cal.–Exp.)/Exp.} x 100

● Control Rod

Fig.16 Radial Flux Distribution of U, Pu Checkerboard Core (DCA)

Table 1 Fuel Composition

Isotope	Weight Fraction in Fuel Pu	E.U
U-235	0.00705	0.015
U-238	0.98544	0.985
Pu-239	0.00435	---
Pu-240	0.00180	---
Pu-241	0.00105	---
Pu-242	0.00029	---

Table 2 Variation of effective absorption cross section with Void Fraction

$\int_0^{0.625ev} \Sigma_a^i \phi dE / \int_0^{0.625ev} \phi dE$ (with CLUSTER code)

Fuel	UO_2			$PuO_2 - UO_2$		
Void Fract.	0 %	100 %	Difference	0 %	100 %	Difference
U^{235}	1.222(-1)	1.270(-1)	4.8(-3)	5.824(-2)	6.187(-2)	3.6(-3)
U^{238}	3.479(-2)	3.597(-2)	1.2(-3)	3.530(-2)	3.722(-2)	1.9(-3)
Pu^{239}	-----	-----	-----	1.003(-1)	9.304(-2)	-7.3(-3)
Pu^{240}	-----	-----	-----	7.692(-3)	8.028(-3)	3.4(-4)
Pu^{241}	-----	-----	-----	2.395(-2)	2.353(-2)	-4.2(-4)
Pu^{242}	-----	-----	-----	7.310(-5)	7.691(-5)	3.8(-6)

Table 3 Macroscopic Absorption Cross Section and Thermal Flux in 0% Void Lattice (with CLUSTER-code)

	UO_2 Lattice			$PuO_2 + UO_2$ Lattice		
	ϕ	$\Sigma a (cm^{-1})$	Total Absorption (Ratio)	ϕ	$\Sigma a (cm^{-1})$	Total Absorption (Ratio)
Fuel	1.363	1.570-1	.7482 (1.00)	1.511	2.256-1	.7840 (1.00)
Coolant	1.618	9.707-3	.0565 (.0755)	1.992	9.756-3	.0443 (.0565)
Lattice Average	2.463	9.687-3	1.00	3.298	1.100-2	1.00

Table 4 Control Rod Worth of U-Pu 2 Region Core (DCA)

Void (%)	Core No.	Experimental Control Rod		Calculational Value			Exp. Value Rod Worth ($)	C/E-1 (%)
		Number	Position in the Core	ΔK/K (%)	Beff (%)	Rod Worth ($)		
0	A-0-4	0		0.0	0.56_0			
	A-1	1	(5B7)	0.21	0.55_8	0.38	0.37±0.03	+2.70
	A-2	1	(1B5)	0.74	0.56_2	1.32	1.34±0.07	−1.49
	A-3	1	(1B1)	1.43	0.57_3	2.50	2.65±0.12	−5.66
	A-4	2	(1B5), (1D5)	1.74	0.56_4	3.09	2.94±0.14	+5.10
	A-5-3	4	(5A1), (1B5), (5C1), (1D5)	4.90	0.56_7	6.88	7.29±0.33	−5.62
	A-6	8	(5A1), (1B5), (5C1), (1D5) (7A5), (5B7), (7C5), (5D7)	4.97	0.55_0	9.04	9.15±0.41	−1.20
100	B-0-5	0		0.0	0.58_2			
	B-3	1	(1B1)	1.51	0.59_1	2.56	3.29±0.10	−2.19
	B-4	2	(1B5), (1D5)	2.03	0.58_4	3.48	4.26±0.13	−8.31
	B-5-2	4	(5A1), (1B5), (5C1), (1D5)	4.42	0.58_8	7.52	9.65±0.29	−22.07
	B-6	8	(5A1), (1B5), (5C1), (1D5) (7A5), (5B7), (7C5), (5D7)	6.06	0.56_9	10.65	13.16±0.40	−19.07

Table 5 Control Rod Reactivity Worth for DCA Core

Void (%)	Control Rods Position	Control Rods Worth (%)		C/E
		ρ_{CR}^{Exp}; Experiment	ρ_{CR}^{cal}; Calculation	
0	1B1	1.09$_4$	1.19$_0$	1.08$_8$
	5B7	0.24$_9$	0.26$_6$	1.06$_8$
	1B5	0.65$_2$	0.79$_7$	1.08$_4$
	1B5 + 1D5	1.56$_5$	1.66$_8$	1.06$_6$
	5A1+1B5+5C1+1D5	3.59$_9$	3.69$_4$	1.02$_6$
30	1B1	1.05$_1$	1.23$_9$	1.17$_9$
	5B7	0.24$_0$	0.27$_9$	1.16$_3$
	1B5	0.62$_2$	0.73$_8$	1.18$_6$
	1B5 + 1D5	1.50$_1$	1.73$_6$	1.15$_7$
	5A1+1B5+5C1+1D5	3.45$_0$	3.83$_6$	1.12$_2$
70	1B1	1.23$_6$	1.33$_9$	1.08$_3$
	5B7	0.29$_3$	0.30$_6$	1.04$_4$
	1B5	0.74$_1$	0.80$_3$	1.08$_3$
	1B5 + 1D5	1.78$_1$	1.87$_9$	1.05$_1$
	5A1+1B5+5C1+1D5	3.96$_7$	4.13$_1$	1.04$_1$
100	1B1	1.61$_0$	1.51$_7$	0.94$_2$
	5B7	0.42$_0$	0.36$_1$	0.86$_0$
	1B5	0.99$_6$	0.92$_6$	0.93$_6$
	1B5 + 1D5	2.33$_1$	2.13$_2$	0.91$_5$
	5A1+1B5+5C1+1D5	5.17$_4$	4.62$_4$	0.89$_4$

Appendix

Input Data of Comparison Cases (from reference (4))

Two kinds of fuel, Pu mixed oxide and slightly enriched U fuel, for 28-rods cluster are selected in order to estimate contribution of Pu on void reactivity.

Input data of comparison cases are as follows.

INPUT DATA of COMPARISON CASES

FUEL CLUSTER

(i) 28 Fuel Rods/cluster in 3 circular rings

Ring	No. of Elements	Pitch Circle Radius of Fuel Rod Centres (cm)
1	4	1.32
2	8	2.96
3	16	4.76

(ii) Element Description

Zone	I.D. (cm)	O.D. (cm)	Material	Density (g/cc)	Temperature (°C)
Fuel Rod	---	1.447	UO_2-PuO_2	10.271	600
Void Space	1.447	1.478	Void	---	---
Sheath	1.478	1.646	Zry-2	7.57	300

(iii) Fuel Composition

Isotope	Weight Fraction in Fuel	
	Pu	E.U
U-235	0.006221	0.013222
U-238	0.868695	0.868266
Oxygen	0.118467	0.118512
Pu-239	0.003838	---
Pu-240	0.001588	---
Pu-241	0.000926	---
Pu-242	0.000255	---

(iv) Structural Tie Rod

Four tubes of Zircaloy-2 (6.57 g/cm^3) with inner radius of 0.28 cm and outer radius of 0.35 cm are located on the ring with radius of 3.44 cm.

CHANNEL

Zone	I.D. (cm)	O.D. (cm)	Material	Density (g/cc)	Temperature (°C)
Pressure Tube	11.78	12.64	Zr-2.5w/o Nb	6.57	285
CO_2-Gap	12.64	14.94	CO_2	---	170
Calandria Tube	14.94	15.24	Zry-2	6.57	60

MODERATOR

D_2O (99.65 mol %), 60°C, 1.090 g/cc

OTHER

(i) Channels on square lattice pitch of 24.0 cm

(ii) Coolant temperature of 285 °C

(iii) Assume bare core, axial buckling = 0.587×10^{-4} cm^{-2}

radial buckling = 1.166×10^{-4} cm^{-2}

Note: coolant material, H_2O

References

(1) S. SHIMA, S. SAWAI, "The FUGEN Project", Can. Nucl. Ass. Ann. Conf. 204 (1973).

(2) D.L. DELP et al., "FLARE, a Three-Dimensional Boiling Water Reactor Simulator", GEAP-4598, General Electric Co. (1964).

(3) R.K. HALING, "Operating Strategy for Maintaining an Optimum Power Distribution through Life", TID-7672 (1963).

(4) H. KATO, S. OHTERU, M. MATSUMOTO, "Effects of Pu on Void Reactivity", Meeting on Void Coefficient of Heavy Water Moderated BLWRs, Paris (1972).

(5) Y. WATARI, H. KATO, "Nuclear Design of Prototype Heavy Water Reactor (FUGEN)", ibid.

(6) T. HAGA, H. KATO, Can. Nucl. Ass. Ann. Conf. TS-3 (1973).

(7) H. SAKATA, Y. HACHIYA, et al., Trans. Am. Nucl. Soc., 16, 267 (1973).

(8) Y. MIYAWAKI, H. KATO, "Heavy Water Critical Experiments on Pu Utilization in ATR FUGEN", IAEA Panel, Karlsruhe (1974).

(9) K. SHIBA, K. IIJIMA, et al., Trans. Am. Nucl. Soc., 21, 467 (1975).

(10) T. WAKABAYASHI, Y. HACHIYA, ibid., 466 (1975).

(11) M. MATSUMOTO, T. HAGA, et al., ibid., 466 (1975).

(12) K. YAMAMOTO, K. KURIHARA, et al., J. Nucl. Sci. Tech. 9,705 (1972).